SciMedCentral

Journal of Drug Design and Research

Research Article

A PCSK9 Antibody and FGF21 Dual Target Conjugate for Treatment of MASH and Hypercholesterolemia

Xujia Wang[1,2#], Qin Meng[1,2#], Aijuan Jia[2], Dandan Song[2], Shaokang Ma[2], Wei Li[2], Zhuobing Zhang[2], Christopher Goldring[3], Hui Feng[4] and Mu Wang[1]*

[1]*Academy of Pharmacy, Xi'an Jiaotong-Liverpool University, China*
[2]*Department of Analytical Science, Shanghai Junshi Biosciences Co., Ltd, China*
[3]*Centre for Drug Safety Science, Department of Molecular and Clinical Pharmacology, University of Liverpool, UK*
[4]*Shanghai Anlingke Biopharmaceutical Co., Ltd, China*
[#]*Xujia Wang and Qin Meng contributed equally to this work*

***Corresponding author**
Mu Wang, Academy of Pharmacy, Xi'an Jiaotong-Liverpool University, 111 Ren'ai Road, SD334F Suzhou, Jiangsu 215123, Tel: +86-0512-8818 4673; China

Submitted: 24 February 2025
Accepted: 05 March 2025
Published: 10 March 2025
ISSN: 2379-089X

Keywords
- Efruxifermin
- PCSK9 antibody
- Conjugate
- MASH
- Hypercholesterolemia

Abstract

Metabolic dysfunction-associated steatohepatitis (MASH), for which there is almost no available medicine, could be a life-threatening disease. A lot of candidates have been tested in preclinical and clinical trials, such as Fc-FGF21 (Efruxifermin, Akero Therapeutics), which can reduce triglyceride significantly in MASH patients, but has little effect on low-density lipoprotein cholesterol (LDL-c) level. Several proprotein convertase subtilisin/kexin type 9 (PCSK9) antibodies which can reduce LDL-c have been approved for hypercholesterolemia, such as Alirocumab and Evolocumab. Protein engineering was used to construct a PCSK9 antibody and FGF21 conjugate. Physiochemical, in vitro and in vivo studies were finished to validate the roles of this candidate. We observed that PCSK9 antibody linked FGF21 had similar efficacy with positive control Fc-FGF21 in 3D NAC-Organ model and MASH mouse model. We also observed this conjugate had significant effect in humanized PCSK9 mouse, which had high level of LDL-c. This was the first report in which roles of PCSK9 antibody linked FGF21 were investigated together and candidate showed supposed dual functions in two different mouse models. Taken together, a candidate drug for MASH and hypercholesterolemia had been successfully developed. In future, animal study in monkey or human will be done to confirm its multifunctional efficacy and synergistic effect further.

INTRODUCTION

Although U.S. Food and Drug Administration (FDA) has approved resmetirom (a small molecule thyroid hormone receptor beta agonist) as the first drug for treatment of metabolic dysfunction-associated steatohepatitis (MASH) or non-alcoholic steatohepatitis (NASH) in 2024 [1,2]. MASH still remains unmet clinical needs. Metabolic dysfunction-associated steatotic liver disease (MASLD) or non-alcoholic fatty liver disease (NAFLD) is a prevalent disease, associated with obesity, dyslipidemia and type 2 diabetes mellitus (T2D). MASH is a serious form of MASLD and is a potential serious disease, which has almost no available medicine treatment today [3]. Steatosis, inflammation, fibrosis and ballooning are typical characteristics of MASLD and MASH [4]. The global prevalence of MASLD is about 25% in adults and lean individuals can also develop MASLD [5].

Fibroblast growth factor 21 (FGF21), as an endogenous protein, is approximately 100 pg/mL in healthy humans and is increased in MASH patients [6]. It belongs to FGF19 subfamily, and the main secreting tissue is liver [7]. There are two kinds of FGF21 receptor, fibroblast growth factor receptor (FGFR) and β-Klotho (KLB) [8] and several FGF21 analogs have been designed and validated in preclinical or clinical trials. Efruxifermin (AKR-001 or AMG 876) is a fusion protein in which Fc fragment of antibody is linked to FGF21 with amino acid mutation, developed by Akero Therapeutics (South San Francisco, USA) [9]. Pegozafermin is a glycoPEGylated FGF21 analog, which is in clinical trials for MASH or severe hypertriglyceridemia (SHTG) treatment, developed by 89bio, Inc. (Herzliya, Israel) [10]. There are other FGF21 candidates, such as Pegbelfermin (BMS-986036, Bristol-Myers Squibb) [11], LY2405319 (Eli Lilly) [12], PF05231023 (Pfizer Inc.) [13], BOS-580 (Novartis Pharmaceuticals) [14]. Our previous work has shown that how to develop a biosimilar of Fc-FGF21[15].

As a member of serine proteinases termed proprotein

convertases, proprotein convertase subtilisin/kexin type 9 (PCSK9) [16], which can bind with low-density lipoprotein receptor (LDLR) and down-regulate LDLR at the cell surface, has been confirmed as an effective target for hypercholesterolemia or hyperlipidemia treatment. Two monoclonal antibodies, Alirocumab and Evolocumab have been approved by the U.S. Food and Drug administration [17-19]. Several antibodies have entered into clinical trials, such as bococizumab [20], a humanized monoclonal antibody (mAb).

Fc-FGF21 has a longer half-life of 3-3.5 days [3] compared to 2 hours of wild type FGF21 [6] and could reduce triglyceride significantly. It also has some promising clinical data with a good chance to be approved by the Food and Drug Administration authorities in the future [3]. PCSK9 antibody can reduce low-density lipoprotein cholesterol (LDL-c). In this study, *N*-terminal of FGF21 (amino acid sequence is the same as Efruxifermin) was linked to *C*-terminal of PCSK9 antibody's heavy chain (a new molecule JS from Shanghai Junshi Biosciences Co., Ltd, which has a weak affinity with mouse PCSK9, but a high affinity with human or monkey PCSK9) with GGGGS GGGGS GGGGS linker to form a single chain amino acid sequence and could be expressed directly just like a heavy chain of traditional antibody. This new candidate drug was supposed to have dual functions or synergistic effect for treatment of MASH and hypercholesterolemia together and similar half-life with Fc-FGF21. This protein was expressed and purified, physiochemical characteristics were analyzed, as well as ELISA, cell-based luciferase reporter assay, 3D MASH model, MASH mouse model and B6-hPCSK9 mouse model were used to evaluate its bioactivity and efficacy.

MATERIALS AND METHODS

Reagents

Fc-FGF21, JS-FGF21, JS were expressed by Shanghai Junshi Biosciences Co., Ltd (Shanghai, China), JS was expressed for former project.

3D NAC-Organ model

MASH 3D NAC-Organ model was provided by Puheng technology (Suzhou, China).

Animals

MASH mice with Dyets AMLN feed were purchased from Charles River, B6hPCSK9 mice with western diet D12079B (SYSE BIO, China) were purchased from

GemPharmatech (China), and all mouse studies were conducted at Suzhou Frontage New Drug Development Co., Ltd (China) and approved by the Institutional Animal Care and Use Committee. Mice were maintained in rooms with a 12-hours light/dark cycle, temperature between 20 and 26 ℃ and humidity between 40 to 70%. Mice had free access to food and water.

Protein expression and purification

The DNA encoding the Fc-FGF21 and JS-FGF21 was synthesized by GENEWIZ (Suzhou, China), cloned into HX1 vector (Shanghai Junshi Biosciences Co., Ltd.) for HEK293 (Thermo-Fisher Scientific) expression by restriction enzymes.

After cell culture, soluble proteins were purified by protein A chromatography (rProtein A, MabSelect SuRe, GE Healthcare) by elution buffer (citrate buffer solution, pH 3.8-3.9). Finally, sample buffer was changed to DPBS (Gibco) by ultrafiltration. Sodium dodecyl sulfate-polyacrylamide gel electrophoresis (SDS-PAGE)

SDS-PAGE analysis of the samples was carried out under reducing and nonreducing conditions in 4-12% pre-cast polyacrylamide gels (180-9217H, Tanon). For reducing conditions, samples had final concentration 1mg/mL containing 2 μL NuPAGE™ Sample Reducing Agent (10X, NP0009, Invitrogen) and 5 μL NuPAGE™ LDS Sample Buffer (4X, NP0007, Invitrogen) with final volume of 20 μL. For nonreducing conditions, 20 μg of each sample was first diluted with ultrapure water to 15μL, then mixed with 5 μL NuPAGE™ LDS Sample Buffer (4X). Gels were stained with 0.125% Coomassie blue R250. It was scanned and analyzed by using Image Lab software (Bio-Rad, version 5.0).

Size-exclusion chromatography (SEC)-HPLC analysis

SEC-HPLC was conducted using U3000 HPLC instrument (Thermo-Fisher Scientific) with TSKgel G3000SWxl column (7.8x300 mm, 5 μm, TOSOH). Mobile phase was phosphate buffer (50 mM PB, 300 mM NaCl, pH 7.0).

Mass spectrometry (MS) analysis

MS analysis was carried on a Vanquish Flex UHPLC system (Thermo-Fisher Scientific) coupled to a Q Exactive Plus orbitrap Mass spectrometer (Thermo-Fisher Scientific). A reversed-phase (RP) column (Waters™ BioResolve™ RP mAb polyphenyl column, 450 Å, 2.7 μm, 2.1x150 mm, Waters Corporation) was used. The deconvolution analysis to the raw mass spectra for molecular weight (MW) determination was performed with BioPharma Finder 3.2 software (Thermo-Fisher Scientific).

Approximately 50 µg of protein was dissolved in 100 µL of water. The PNGaseF enzyme (P0704L, New England BioLabs) was added to the sample and it was incubated at 37 °C for four hours. Reduced the sample by addition of 2 µl of 0.5 M DTT, incubated for 30 min at 37 °C.

The initial elution mobile phase contained 80% solvent A (0.10% formic acid + 0.02% trifluoroacetic acid in water) and 20% solvent B (0.08% formic acid + 0.02% trifluoroacetic acid in acetonitrile). After equilibrating with initial mobile phase for 2 min, the linear gradient to solvent B climbed to 32% in 2 min, then to 37% in 8 min, and maintained for 3 min at 90% at a constant flow rate of 0.4 mL/min. For MS scanning, the mode was set as positive, spray voltage was 3.8 kV and sheath gas was 35 Arb. The scan range was 500 to 3,500 m/z.

Enzyme-linked immunosorbent assay (ELISA)

Human FGFR1 (10616-H08H) and mouse FGFR1 (50186-M08H) were purchased from Sino Biological (Beijing, China). Human KLB (RPH756Hu01) and mouse KLB (RPH756Mu01) were purchased from Cloud-clone (Wuhan, China). Other reagents were obtained from Shanghai Junshi Biosciences Co., Ltd (Shanghai, China).

For PCSK9 binding ELISA, Ninety-six-well polystyrene microtiter plates were coated by human PCSK9. After incubation, washing, blocking and washing, samples are added. After washing, Anti-human IgG (Fc specific)–peroxidase antibody produced in goat (A0170, Merck) was added. After color developing and ending, microplate reader was used to read numbers under 450 nm.

For FGFR1 and KLB binding ELISA, Ninety-six-well polystyrene microtiter plates were coated by FGFR1 or KLB. After incubation, washing, blocking and washing, samples are added. After washing, primary antibody human FGF21 antibody in goat (AF2539, R&D Systems) was added. After washing, secondary antibody anti-goat antibody (HAF109, R&D Systems) was added. After color developing and ending, microplate reader was used to read numbers under 450 nm.

LDL uptake assay in HepG2 cell

HepG2 cells (ATCC) were plated at $2.5x10^5$ cells per mL, 80 µL/well. After incubation at 37 °C, 7% CO_2 for 18 hrs, gradient-diluted samples were added, 10 µL/well, incubation 37 °C, 7% CO_2 for 0.5 hr, then 10 µL/well Human PCSK9 was added, incubation 37 °C, 7% CO_2 for 5 hrs. BODIPY FL Low-density lipoprotein (25200072, Thermo-Fisher Scientific) was added, 10 µL/well, incubation 37 °C, 7% CO_2 for 18 hrs. Removed supernatant and 100 µL per well PBS was added and removed. M5 (Molecular Devices) was used to read fluorescent (Ex=480nm, Em=520 nm).

ELK luciferase assay

HEK293-KLB/ELK1-LBD/GAL4-LUC cells (Wuhan ConradBio, China) were plated at $2.2*10^5$ cells per mL, 90 µL/well. After incubation at 37°C, 5% CO_2 for 18 hrs, gradient-diluted FGF21 was added, 10 µL/well, incubation 37°C, 5% CO_2 for 6 hrs, then 50 µL supernatant was discarded and 50 µL ONE-Glo (E6120, Promega) was added.

M5 (Molecular Devices) was used to read luminescence.

3D NAC-Organ study

Primary human hepatocytes (PHH), liver sinusoidal endothelial cells (LSEC), hepatic stellate cells (HSC), Kupffer cells (KC) are purchased from LV BioTech (Shenzhen, China), 1500 PHH:692 LSEC:462 HSC:346 KC are cocultured to form 3D liver model for 48 hrs which is then induced to 3D MASH model for 10 days by Puheng technology (Suzhou, China). Drugs are added at day 4. Supernatants are collected at day 6 for IL-6 test (Zhuochai Biology, China). Liver microspheres are collected for total triglyceride (Applygen, China), Hematoxylin eosin (Servicebio, China) and Sirius red (HEAD biotechnology, China) staining at day 12.

Final concentration of positive control Fc-FGF21 was 1 µg/ml, JS 1.55 µg/ml. JSFGF21 was set into 3 groups, 20, 2 and 0.2 µg/ml. All of them had same molar concentration, 10 nM.

Animal studies

All mouse studies were conducted at Suzhou Frontage New Drug Development Co., Ltd (China) and were approved by Institutional Animal Care and Use Committee, IACUC No. AN-2024-S101. Mice were housed in individually ventilated cage (IVC) systems at constant temperature (20-26°C) and humidity (40-70%) with 1 animal per cage. Animals had free access to sterile drinking water, day and night alternation.

In order to compare candidate drug JS-FGF21 with positive control Fc-FGF21, male C57BL/6J mice [8] (26 weeks old, purchased from Charles River) were randomized to 3 groups, MASH vehicle group, Fc-FGF21 and JS-FGF21 and fed with AMLN feed (Charles River). Every group had 5 mice and the total number was 15, which was a common setting for every group. Dosing or blood collection were completed according to a fixed order very time. Drugs were administrated by intraperitoneal

administration once a week for 8 weeks. Body weight was examined every 3-4 days. TC, TG, AST, ALT, HDL-c and LDL-c were tested every 2 weeks. Before blood collection, animals were fasted for 16 hrs. Animals were bleeding by saphenous vein puncture. Blood was kept at RT for 2 hrs before centrifuging at 5,000xg for 5 min for serum extraction. At endpoint, animals were sacrificed by a humane euthanasia (90% carbon dioxide anesthesia at the speed of 30% volume of euthanasia box per minute and cervical dislocation) and liver weight was recorded. If severe dehydration, impaired mobility, ananastasia happened, study would be terminated. No data was excluded in all data. For authors, we knew the group allocation, but didn't interfere.

Prism 8.3 was used to analyze data. Mean and S.D. were reported.

In order to confirm dual functions of candidate, B6-hPCSK9 mice (high level of LDL-c) were operated and divided into two groups, vehicle group and JS-FGF21 group.

Drugs were administrated by intraperitoneal administration once a week for 4 weeks. Body weight was examined every 3-4 days. TC, TG, AST, ALT, HDL-c and LDL-c were tested every 2 weeks.

Statistical analysis

Prism 8.3 was used to draw figures. All data was means ± standard deviation (S.D.). Values were compared using Student's paired t-test. $p < 0.05$ was considered as statistically significant.

RESULTS AND DISCUSSION

Expression of Fc-FGF21 and JS-FGF21

Fc-FGF21 and JS-FGF21 were expressed by human embryonic kidney 293 (HEK293) cells. Under reduced condition, Fc-FGF21's molecular weight was about 54.9 kDa, JS-FGF21 was divided into heavy chain and light chain, molecular weight 80.3 kDa and 30.4 kDa, respectively. Under non-reduced condition, Fc-FGF21's molecular weight was about 104.4 kDa, JS-FGF21's molecular weight was about 241.7 kDa (Figure 1). Results of SDS-PAGE were consistent with theoretical values.

Results of SEC-HPLC showed all of them were very pure, main peak more than 90.0%, with low aggregate (Figure 2).

Molecular weight confirmation by Mass spectrometry

Although results of SDS-PAGE had confirmed JS-FGF21 was expressed correctly. Mass spectrometry had been used to confirm it further. After deglycosylation and reduced, JS-FGF21 was reduced to two chains, the light chain JS-FGF21 was about 23,544 Da, the heavy chain of JS-FGF21 was about 68345 Da, which were consistent with theoretical value 23,543 Da and 68,347 Da, respectively (Figure **3**).

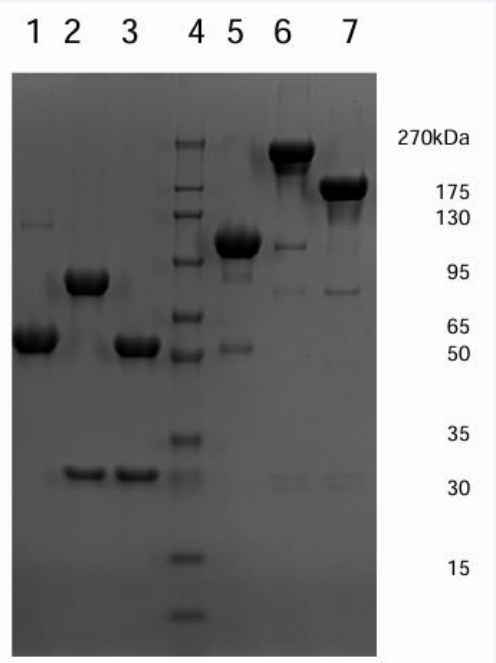

Figure 1 SDS-PAGE result of Fc-FGF21, JS-FGF21, and JS. **Lane 1-3**: reduced SDSPAGE; **Lane 5-7**: non-reduced SDS-PAGE; **Lane1 and 5**: Fc-FGF21; **Lane 2 and 6**: JSFGF21; **Lane 3 and 7**: JS; **Lane 4**: molecular weight markers.

In vitro evaluation

In order to evaluate if JS-FGF21 retained the function of PCSK9 antibody, human PCSK9 binding ELISA was performed. Fc-FGF21 couldn't bind with PCSK9, whereas JS and JS-FGF21 could bind with PCSK9, respectively. They had similar EC50 (0.01 nM), which indicated that JS-FGF21 retained affinity of PCSK9 (Figure 4).

To evaluate if JS-FGF21 retained the function of FGF21, human FGFR1, mouse FGFR1, human KLB and mouse KLB binding ELISA were carried out. JS couldn't bind with any of them, whereas Fc-FGF21 and JS-FGF21 could bind with human FGFR1, mouse FGFR1, human KLB, and mouse KLB. They had a similar trend, which suggested that JS-FGF21 retained affinity of FGFRs, even better than Fc-FGF21 (Figure **5**).

Two cell-based assays were established to evaluate bioactivities of PCSK9 antibody and FGF21 further. In HepG2 cells, when PCSK9 was added, LDLR would be reduced, and uptake of LDL-c decreased. On the contrary, when PCSK9 antibody was added, PCSK9 decreased, and uptake of LDL-c increased. Fc-FGF21 had no effect on this

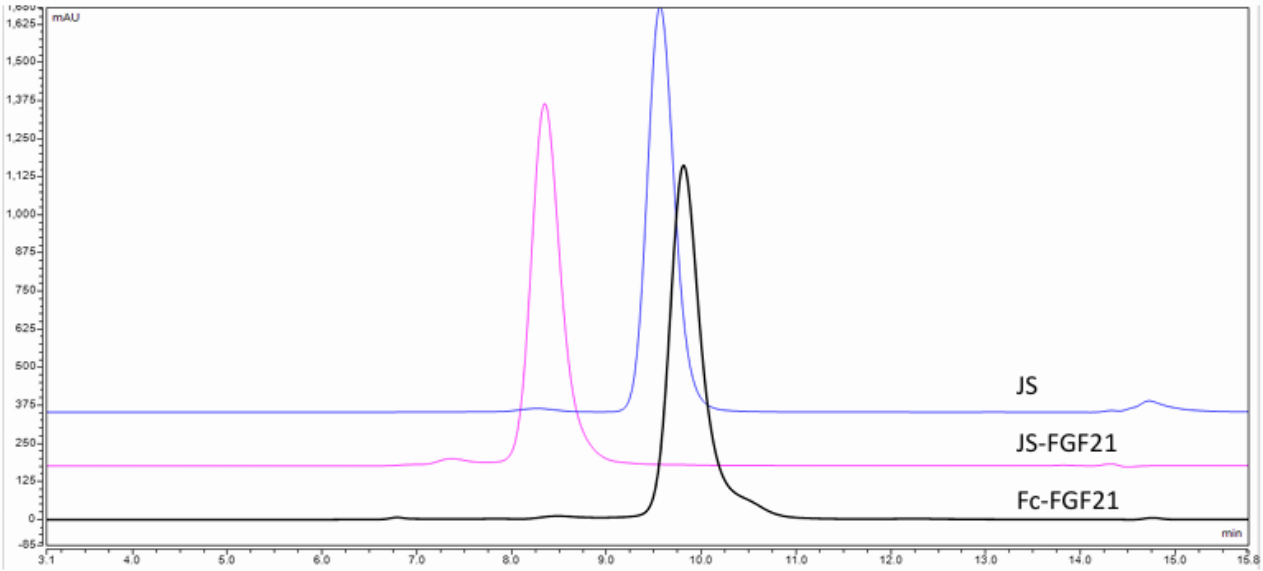

Figure 2 SEC-HPLC result of Fc-FGF21, JS-FGF21, and JS.

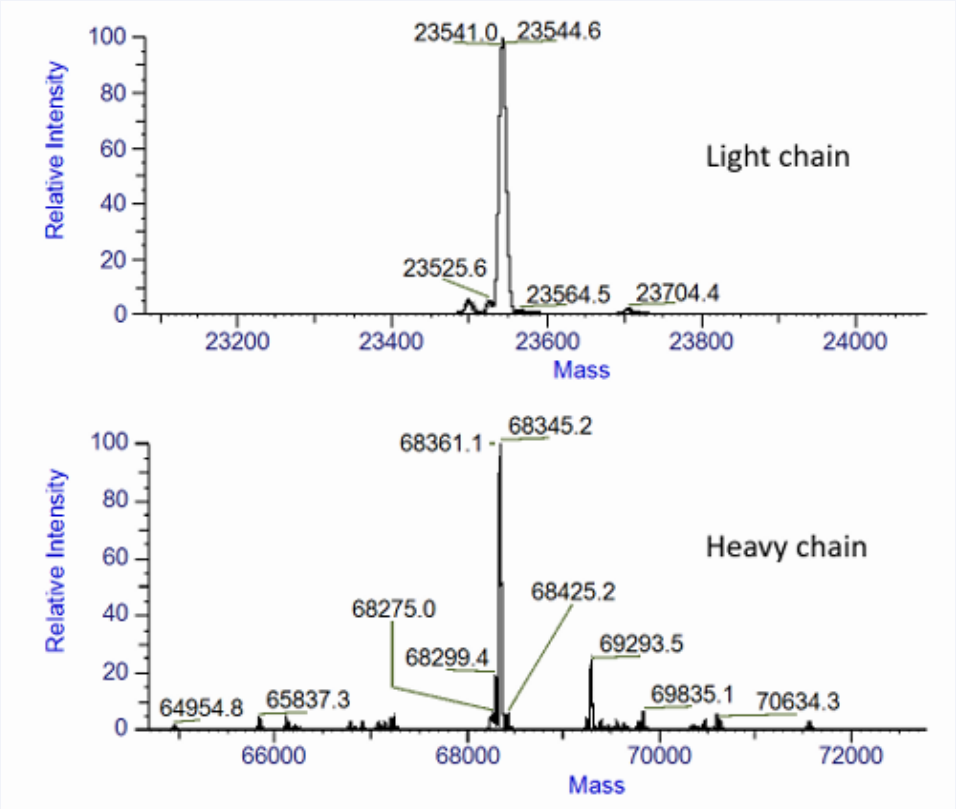

Figure 3 Mass spectrometry results used to identify JS-FGF21. After deglycosylation and reduced, the light chain was about 23544 Da, the heavy chain was about 68345 Da.

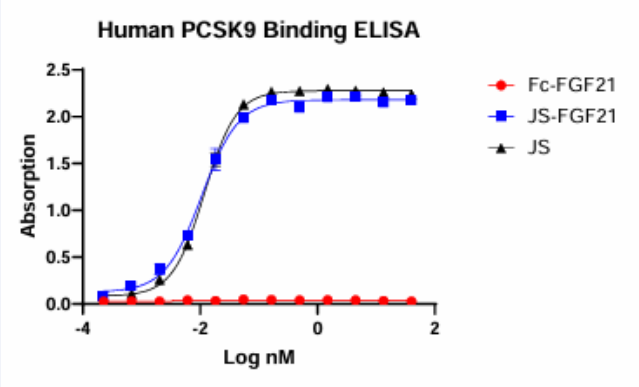

Figure 4 ELISA of PCSK9 antibody's binding with human PCSK9. Fc-FGF21 couldn't bind with PCSK9, but JS-FGF21 and JS could bind with PCSK9, and had similar EC50, about 0.01nM.

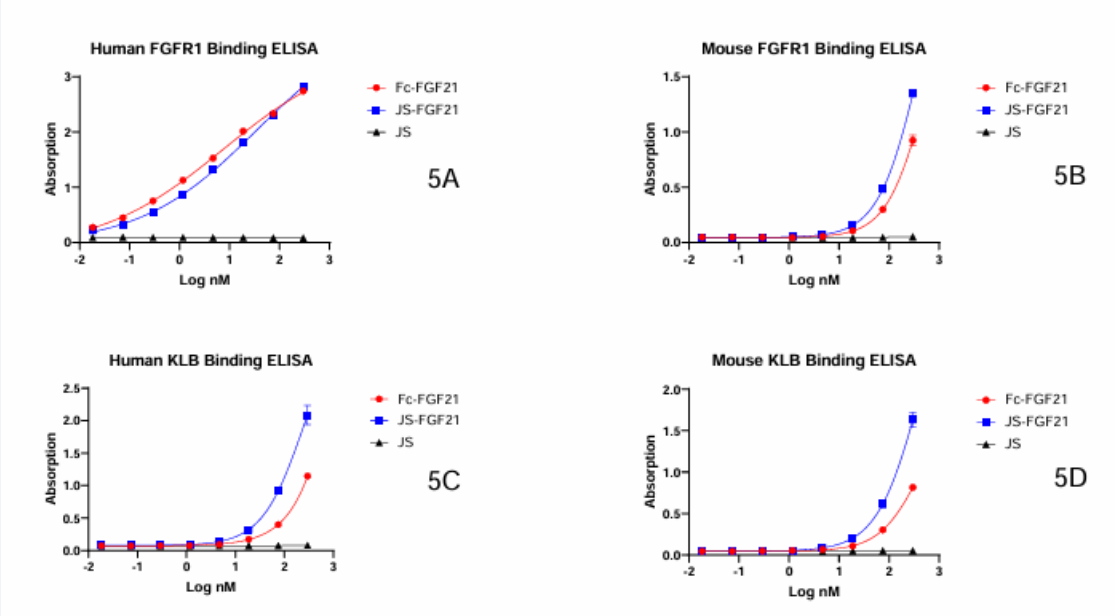

Figure 5 ELISA of FGF21's binding with FGF receptors. **5A**, human FGFR1 binding with FGF21; **5B**, mouse FGFR1 binding with FGF21; **5C**, human KLB binding with

FGF21; **5D**, mouse KLB binding with FGF21. JS couldn't bind with FGFR1 or KLB.

cell model. JS and JS-FGF21 had a similar effect, EC50 was at 0.89 nM and 0.77 nM, respectively (Figure 6), which confirmed the results from ELISA. JS-FGF21 had similar functions of PCSK9 antibody.

In order to evaluate the functions of FGF21 more accurately, KLB/ELK1 luciferase reporter assay was performed in HEK293 cells. When FGF21 was added, ELK1 was phosphorylated and luciferase was expressed. JS couldn't induce expression of luciferase. Fc-FGF21 and JS-FGF21 could increase expression of luciferase with similar EC50, 0.16 nM and 0.21 nM, respectively (Figure 7). JS-FGF21 had similar functions of FGF21.

Efficacy studies in MASH 3D NAC-Organ model

In order to evaluate the functions of Fc-FGF21 further, 3D NAC-Organ liver model was established and induced to MASH model. After drug treatment for 10 days, several parameters were measured.

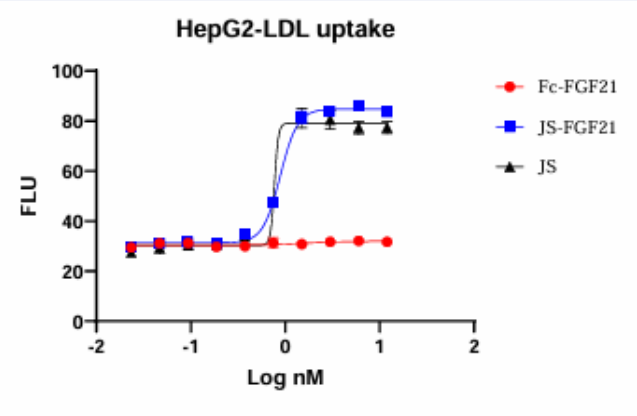

Figure 6 LDL-c uptake experiment in HepG2 cells. The higher concentration of PCSK9 antibody, the more signal of fluorescent. Fc-FGF21 couldn't increase uptake of LDL-c, but JS-FGF21 and JS had similar EC50, 0.89 and 0.77 nM respectively.

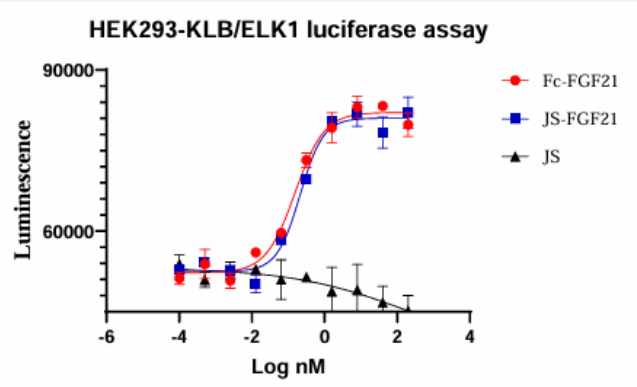

Figure 7 Luciferase reporter assay of FGF21. The higher FGF21 concentration, the more signal of luminescence. Fc-FGF21 and JS-FGF21 had similar EC50 0.16 and 0.21 nM respectively. JS couldn't increase signal.

IL-6 level was elevated in MASH group compared to Lean group from 6.1 pg to 8.3 pg, which indicated that inflammation was induced in this MASH model. After the treatment, IL-6 level was down-regulated in Fc-FGF21 group, JS-FGF21 group and JS group, with similar effect, 5.9 pg in Fc-FGF21, 6.5 pg in JS-FGF21 high dose group, 6.4 pg in JS-FGF21 medium dose group, 7.3 pg in JS-FGF21 low dose group, and 6.9 pg in JS group (Figure 8). JS-FGF21 high dose and medium dose groups had a similar effect with Fc-FGF21 on IL-6 level.

TG level was elevated in MASH group compared to Lean group from 5.8 nM to 7.6 nM (Figure 8). None of the groups could reduce the level of TG, which indicates that TG level was not a sensitive parameter for evaluating FGF21's function in this model.

Results of HE-staining showed MASH group had obvious features of steatosis compared to Lean group. None of the groups could reverse the level of steatosis (Figure 9).

Results of Sirius red staining showed that MASH group had a higher level of fibrosis compared to Lean group (0.04 area percentage versus 0.1 area percentage). Positive control Fc-FGF21 could reverse fibrosis with a reduced area percentage, 0.05 area percentage. Three concentrations of JS-FGF21 had a similar effect to reverse fibrosis, 0.04, 0.04, and 0.03 area percentage, respectively, compared to Fc-FGF21. JS also showed some effect (Figure 8 & 10).

Efficacy studies in MASH mouse model

Before the efficacy studies, PK parameters were investigated by double FGF21 antibodies ELISA (coating recombinant anti-mouse FGF21 antibody, rabbit

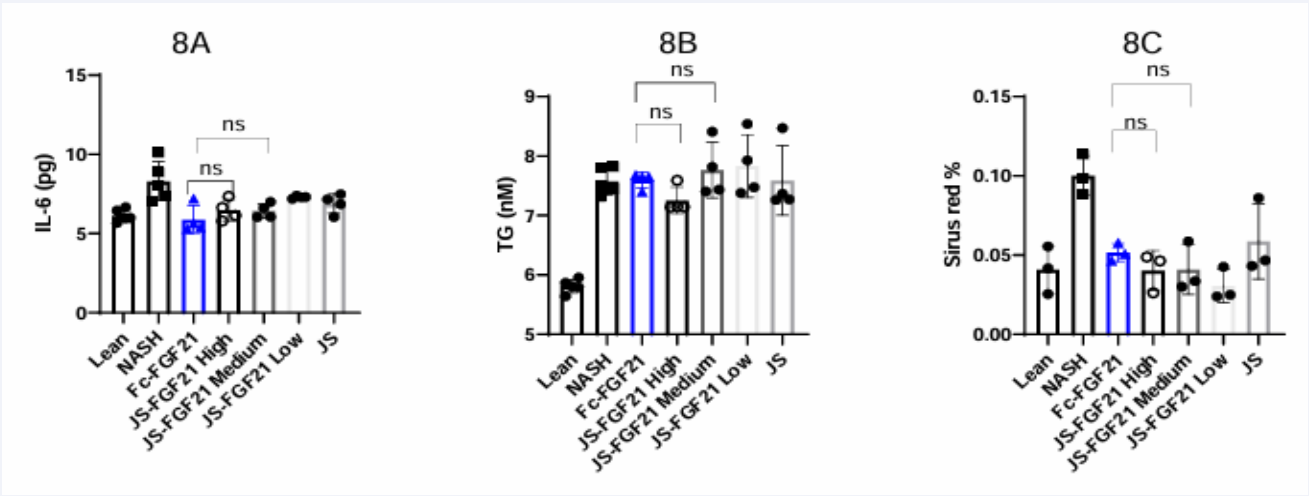

Figure 8 Efficacy study in 3D NAC-Organ model. **8A**, results from IL-6; **8B**, results from triglyceride (TG); **8C**, results from Sirius red staining.

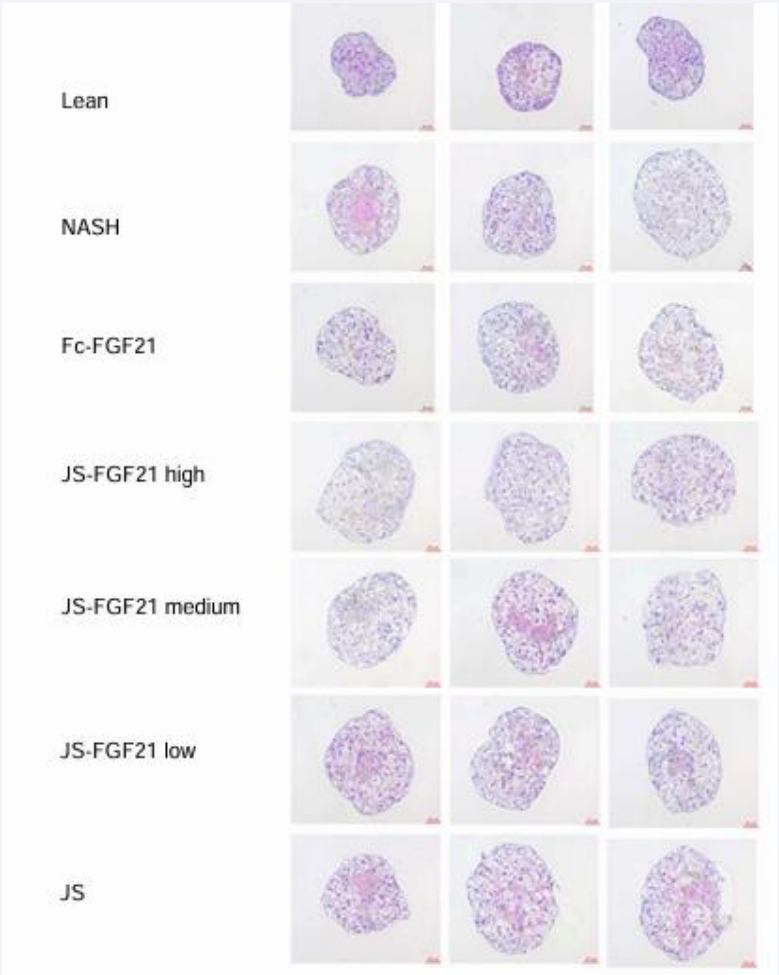

Figure 9 Hematoxylin eosin staining in 3D NAC-Organ model.

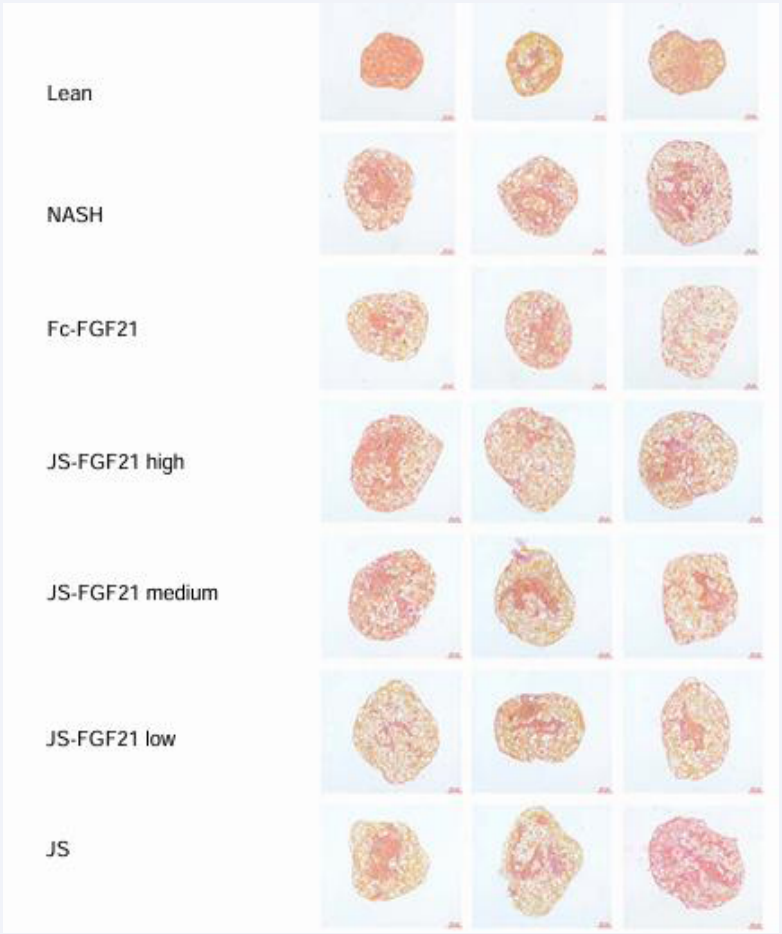

Figure 10 Sirius red staining in 3D NAC-Organ model.

monoclonal antibody, 50421-R005, from Sino Biological; secondary antibody: human FGF-21 antibody from goat, AF2539, R&D and anti-goat IgG HRP Conjugated from Donkey, HAF109, R&D). After dosing by intraperitoneal, intravenous and subcutaneous, respectively, serum of 5 min, 1 hr, 2 hrs, 6 hrs, 24 hrs, 48 hrs, 72 hrs, 96 hrs, and 168 hrs were collected and analyzed. Positive control Fc-FGF21 was only given by intravenous route. Candidate drug JS-FGF21 has a half-life of 1.56 days, a little better than 1.13 days of Fc-FGF21. Other two administration routes have a similar half-life, 1.54 days and 1.78 days, respectively. Thus, administration period was set according to Fc-FGF21 [6], one dosing per week.

In order to evaluate the functions of JS-FGF21 further, study in MASH mouse model was finished. After administration of 8 weeks, body weight declined significantly in Fc-FGF21 and JS-FGF21 group, 29.6 and 30.9 g compared to 38.8 g in vehicle group, this result showed FGF21 had weight loss function which was consistent with references [3, 21]. Candidate JS-FGF21 had similar effect with positive control in area of body weight. Liver weight showed similar trend with body weight. At the endpoint, the average liver weight were 950 mg and 1,058 mg in Fc-FGF21 and JS-FGF21 group, but liver weight in vehicle group was 2,096 mg, which was 2 times heavier than dose group.

AST, ALT, TC and LDL-c had similar results. Fc-FGF21 and JS-FGF21 had similar effect on these parameters, whereas vehicle group had expectant values, see Table 1 and Figs. 11&12. Because PCSK9 antibody had weak affinity with mouse PCSK9, PCSK9 antibody's function was not exhibited in this model.

Efficacy studies in hPCSK9 mouse model

In order to evaluate the functions of JS-FGF21 further, study in hPCSK9 mouse model was finished. After administration of 4 weeks, LDL-c declined significantly in JSFGF21 group, 0.7 mmol/L compared to 1.1 mmol/L

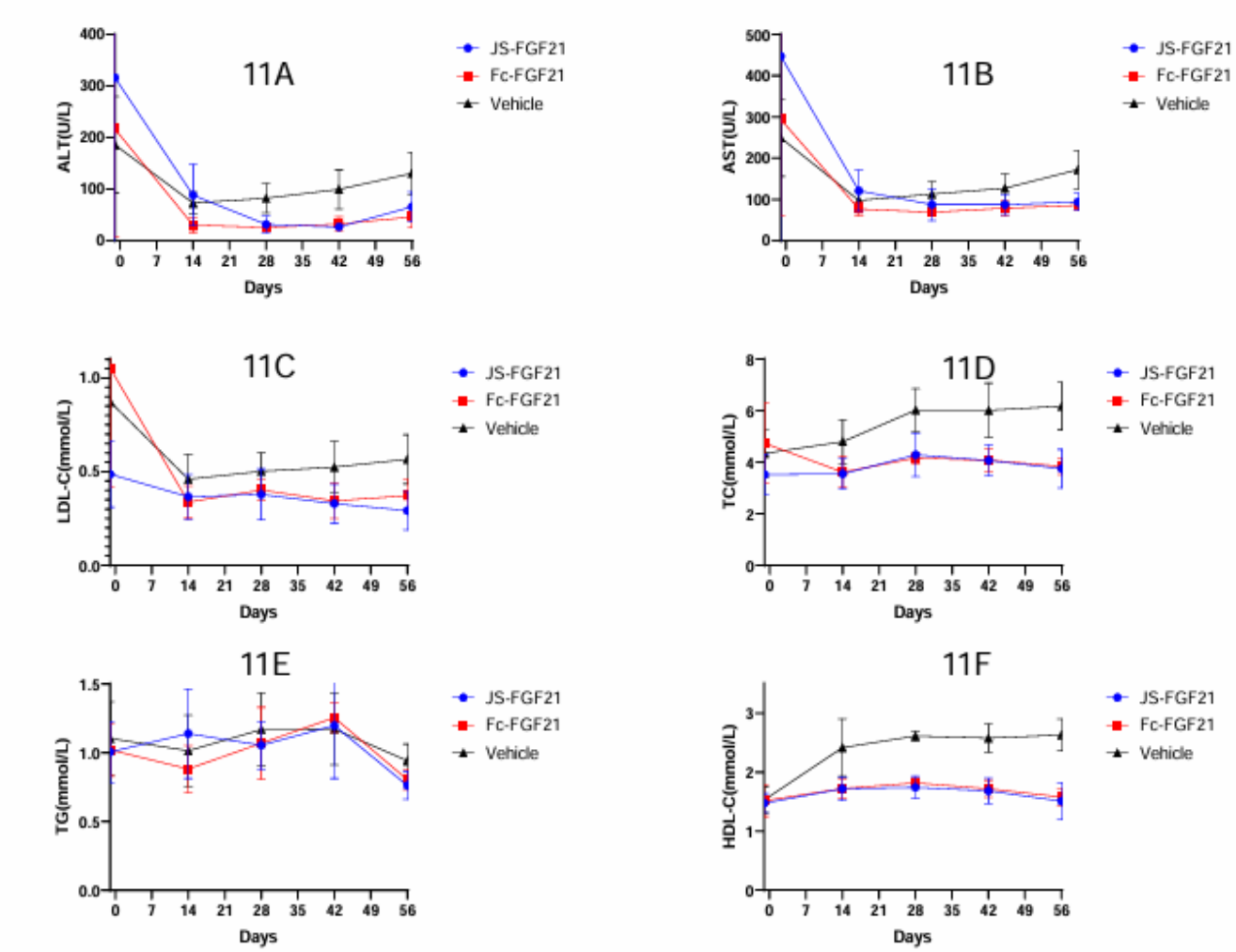

Figure 11 Efficacy study in MASH mouse model. **11A**, ALT curve; **11B**, AST curve; **11C**, LDL-c curve; **11D**, TC curve; **11E**, TG curve; **11F**, HDL-C curve.

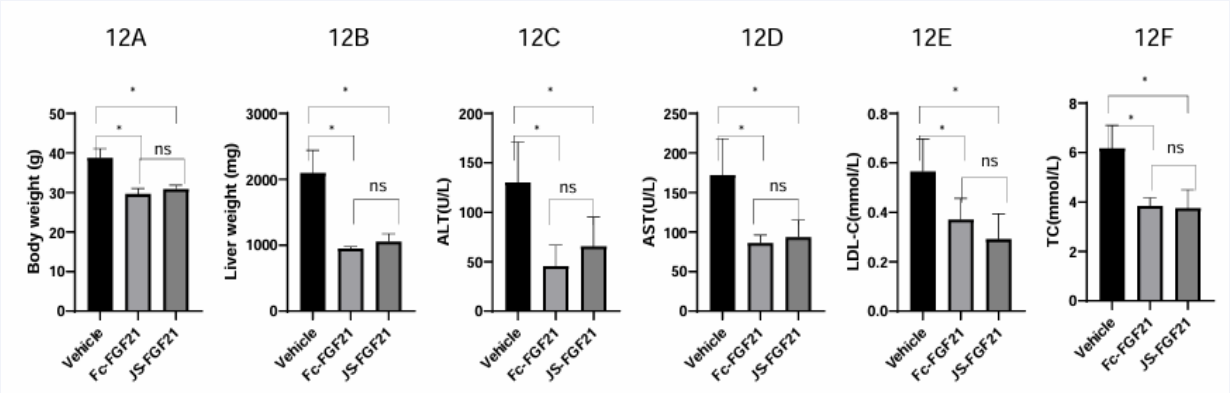

Figure 12 Efficacy study in MASH mouse model. **12A**, endpoint result of bodyweight; **12B**, endpoint result of liver weight; **12C**, endpoint result of ALT; **12D**, endpoint result of AST; **12E**, endpoint result of LDL-c; **12F**, endpoint result of TC.

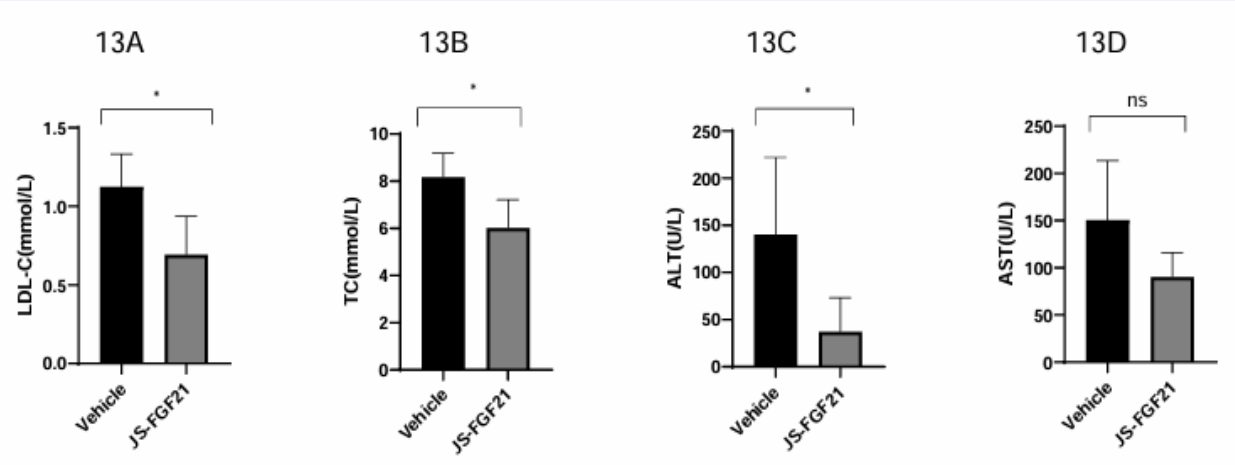

Figure 13 Efficacy study in hPCSK9 mouse model. **13A**, endpoint result of LDL-c; **13B**, endpoint result of TC; **13C**, endpoint result of ALT; **13D**, endpoint result of AST.

Table 1. Average biochemical parameters of endpoint in MASH animal study.

	Vehicle ± SD	Fc-FGF21 ± SD	JS-FGF21 ± SD
Liver weight (mg)	2095.5±346.9	950.4±29.1	1058.1±114.5
Body weight (g)	38.8±2.3	29.6±1.4	30.9±1.0
ALT (U/L)	130.3±40.7	45.7±21.0	65.7±29.6
AST (U/L)	172.1±46.0	86.2±10.2	93.9±21.2
TC (mmol/L)	6.2±0.9	3.8±0.3	3.8±0.7
LDL-c (mmol/L)	0.6±0.1	0.4±0.1	0.3±0.1
HDL-c (mmol/L)	2.6±0.3	1.6±0.2	1.5±0.3
TG (mmol/L)	0.9±0.1	0.8±0.1	0.8±0.1

Table 2. Average biochemical parameters of endpoint in hPCSK9 mouse study.

	Vehicle ± SD	JS-FGF21 ± SD
Body weight (g)	40.9±4.1	38.2±4.6
ALT (U/L)	140.3±81.7	37.4±35.9
AST (U/L)	150.8±62.8	90.4±25.6
TC (mmol/L)	8.2±1.0	6.0±1.2
LDL-c (mmol/L)	1.1±0.2	0.7±0.2

in vehicle group, which was consistent with references [22-24]. TC declined significantly in JS-FGF21 group, 6.0 mmol/L compared to 8.2 mmol/L in vehicle group, ALT declined significantly in JSFGF21 group, 37.4 U/L compared to 140.3 U/L in vehicle group, see Table 2 and Figure 13. Although there was no significant difference in AST, which also showed declined trend. TG, HDL-c and body weight had no differences. Two different animal model confirmed that this dual target candidate had multifunctional efficacy.

CONCLUSIONS

JS-FGF21 was expressed successfully, and there was no significant degradation during the production process. Wild-type FGF21 was easily degraded from its *C* terminal during cell culture [25]. Mass spectrometry confirmed its integrity. JS-FGF21 had both PCSK9 antibody and FGF21's functions, such as PCSK9 binding, FGFR1 binding, and KLB binding. This protein engineering didn't change its *in vitro* bioactivity. Cell-based assays confirmed its potency further. All *in vitro* data showed that JS-FGF21 possessed all functions of PCSK9 antibody and FGF21 respectively.

NAC-Organ MASH model could be a good model to evaluate functions of FGF21 [26]. In this study, IL-6, TG and Sirius red were choosing for evaluation of candidate drugs. Compared to lean group, IL-6 and TG were elevated in MASH model, which meant inflammation and steatosis were induced. Sirius red staining meant fibrosis was induced. All of them elucidated that MASH model was established well. It could be used to evaluate candidate's function. Compared to positive control Fc-FGF21, candidate drug JS-FGF21 had similar effect on MASH treatment.

Animal study should be a more accurate method to evaluate efficacy of candidate drugs before clinical trials. There was not appropriate mouse model to evaluate PCSK9 antibody and FGF21's function together, because of PCSK9 antibody JS had weak affinity with mouse PCSK9. Approved PCSK9 antibodies, such as evolocumab and alirocumab have a weak affinity with mouse PCSK9, 17,000 pM of evolocumab vs. 16 pM of human PCSK9 from the FDA website (https://www.accessdata.fda.gov/drugsatfda_docs/nda/2015/125522Orig1s000TOC.cfm). Most of them use monkey model in preclinical study or hPCSK9 mouse [22].

In this study, mouse MASH model was used to evaluate JS-FGF21's function, but it couldn't reflect PCSK9 antibody's role [27, 28]. This PCSK9 antibody only has strong affinity

with human or monkey PCSK9, mouse model couldn't show PCSK9 antibody's role. Human PCSK9 transgenic mouse was needed. Unfortunately, there was no available PCSK9 transgenic MASH model in the market. So, another mouse model was introduced. High level of LDL-c in hPCSK9 model was also evaluated in this study to confirm JS-FGF21's role, which had shown JS-FGF21 was good candidate for hypercholesterolemia treatment. In order to evaluate multifunctional efficacy or synergistic effect of PCSK9 antibody and FGF21, monkey study or clinical trial were needed further.

FGF21 is not only a candidate for MASH treatment, it also can be a candidate for body weight loss. Today, the most popular medicines for body weight loss is Semaglutide, a GLP-1 receptor agonist [29]. A hypercholesteremia mouse model with high weight maybe a good mouse model to evaluate body weight loss and reducing cholesterol of JS-FGF21, which would reflect if JS-FGF21 has synergistic effect. Hypercholesteremia mice on the market were not enough fat, and they were fed with high fat diet to help gain body weight. Unfortunately, this model failed because they couldn't grow more than 35 grams, which meant this model was hard to evaluate function of body weight loss and lowering LDL-c simultaneously.

Immunogenicity often induces safety problem and is a common phenomenon of recombinant proteins [30]. Different proteins may have different rates of immunogenicity, such as anti-drug antibodies (ADA). Adalimumab as the previous best-selling drug has a high rate of ADA (31.76%) and secukinumab has a low rate of ADA (0.49%) [31]. Thus this candidate may have a high ADA rate caused by PCSK9 antibody and FGF21 with mutation together. Immunogenicity will be paid attention to in future work.

All data had shown that JS-FGF21 was a potential good candidate for MASH and hypercholesteremia treatment. More studies will be done to confirm this hypothesis further in future.

ACKNOWLEDGMENTS

This study was supported by Shanghai Junshi Biosciences Co., Ltd and Xi'an Jiaotong-Liverpool University (XJTLU). We thank Dr. Chao He, Aidi Gao, Yifan Jiang, and the other members of Professor Mu Wang's research group. We thank the scientific staffs of XJTLU Center for Pharmaceutical Analysis (CPA) for Mass spectrometry analysis and the staffs of Wuhan Heyan Biotech for cell lines used in this study. We also thank Minlu Fan, Longjian Xue, Minze Lu, Xueting Li from Shanghai Junshi Biosciences Co., Ltd for their technical assistance.

FUNDING

The research was funded by an internal research fund from Shanghai Junshi Biosciences Co., Ltd.

AUTHORS' CONTRIBUTIONS

Xujia Wang and Qin Meng: conceptualization, investigation, methodology, writing original draft. Aijuan Jia, Dandan Song, Shaokang Ma and Wei Li: methodology and sample preparation. Zhuobing Zhang, Christopher Goldring, Hui Feng and Mu Wang: conceptualization, supervision, review, editing.

All authors approved the final version and agreed to be accountable for all aspects of the work in ensuring that questions related to the accuracy or integrity of any part of the work are appropriately investigated and resolved.

ETHICAL APPROVAL

All mouse studies were conducted at Suzhou Frontage New Drug Development Co., Ltd (China) and were approved by Institutional Animal Care and Use Committee, No. AN-2024-S101.

DATA AVAILABILITY STATEMENT

Materials described in this manuscript including all relevant raw data will be freely available from the corresponding author for non-commercial use upon request.

REFERENCES

1. Michail Kokkorakis, Chrysoula Boutari, Michael A Hill, Vasilios Kotsis, Rohit Loomba, Arun J Sanyal, et al. Resmetirom, the first approved drug for the management of metabolic dysfunction-associated steatohepatitis: Trials, opportunities, and challenges. Metabolism. 2024; 154: 155835.
2. Sanja Borozan, Snežana Vujošević, Dimitri P Mikhailidis, Emir Muzurović. Metabolic Dysfunction-Associated Steatohepatitis and Cardiovascular Disease Prevention: Is Resmetirom Useful?. Curr Vasc Pharmacol. 2024.
3. Stephen A Harrison, Peter J Ruane, Bradley L Freilich, Guy Neff, Rashmee Patil, Cynthia A Behling, et al. Efruxifermin in non-alcoholic steatohepatitis: a randomized, double-blind, placebo-controlled, phase 2a trial. Nat Med. 2021; 27: 1262-1271.
4. Smeuninx, B, E. Boslem, M.A. Febbraio. Current and Future Treatments in the Fight Against Non-Alcoholic Fatty Liver Disease. Cancers (Basel). 2020; 12: 7.
5. Priyanka Bhandari, Amit Sapra, Mohitkumar S, Ajmeri, Christine E Albers, Devanshika Sapra. Nonalcoholic Fatty Liver Disease: Could It Be the Next Medical Tsunami?. Cureus. 2022; 14: e23806.
6. Allegra Kaufman, Lubna Abuqayyas, William S Denney, Erik J Tillman, Tim Rolph. AKR-001, an Fc-FGF21 Analog, Showed Sustained Pharmacodynamic Effects on Insulin Sensitivity and Lipid Metabolism in Type 2 Diabetes Patients. Cell Rep Med. 2020; 1: 100057.

7. Kyle H Flippo, Matthew J Potthof. Metabolic Messengers: FGF21. Nat Metab. 2021; 3: 309-317.

8. Stanislaus S, Hecht R, Yie J, Hager T, Hall M, Spahr C, et al. A Novel Fc-FGF21 With Improved Resistance to Proteolysis, Increased Affinity Toward β-Klotho, and Enhanced Efficacy in Mice and Cynomolgus Monkeys. Endocrinology. 2017; 158: 1314-1327.

9. Stephen A Harrison , Peter J Ruane , Bradley Freilich , Guy Neff , Rashmee Patil, Cynthia Behling, et al. A randomized, double-blind, placebo-controlled phase IIa trial of efruxifermin for patients with compensated NASH cirrhosis. JHEP Rep. 2023; 5: 100563.

10. Moti Rosenstock , Leo Tseng, Andrew Pierce, Elliot Offman, Chao-Yin Chen, R Will Charlton, et al. The Novel GlycoPEGylated FGF21 Analog Pegozafermin Activates Human FGF Receptors and Improves Metabolic and Liver Outcomes in Diabetic Monkeys and Healthy Human Volunteers. J Pharmacol Exp Ther, 2023; 387: 204-213.

11. Arun Sanyal, Edgar D Charles, Brent A Neuschwander-Tetri, Rohit Loomba, Stephen A Harrison, Manal F Abdelmalek, et al. Pegbelfermin (BMS-986036), a PEGylated fibroblast growth factor 21 analogue, in patients with non-alcoholic steatohepatitis: a randomised, double-blind, placebo-controlled, phase 2a trial. Lancet. 2019; 392: 2705-2717.

12. Cong Thuc Le, Giang Nguyen, So Young Park, Dae Hee Choi, Eun-Hee Cho. LY2405319, an analog of fibroblast growth factor 21 ameliorates alpha-smooth muscle actin production through inhibition of the succinate-G-protein couple receptor 91 (GPR91) pathway in mice. PLoS One. 2018; 13: e0192146.

13. Saswata Talukdar, Yingjiang Zhou, Dongmei Li, Michelle Rossulek, Jennifer Dong, Veena Somayaji, et al. A Long-Acting FGF21 Molecule, PF-05231023, Decreases Body Weight and Improves Lipid Profile in Non-human Primates and Type 2 Diabetic Subjects. Cell Metab, 2016; 23: 427-440.

14. Dimitrios D Raptis, Christos S Mantzoros, Stergios A Polyzos. Mantzoros, and S.A. Polyzos, Fibroblast Growth Factor-21 as a Potential Therapeutic Target of Nonalcoholic Fatty Liver Disease. Ther Clin Risk Manag. 2023; 19: 77-96.

15. Xujia Wang, Qin Meng, Aijuan Jia, Yuehua Zhou, Dandan Song, Shaokang Ma, et al. Construction and Expression of Fc-FGF21 by Different Expression Systems and Comparison of Their Similarity and Difference with Efruxifermin by In Vitro and In Vivo Studies. Appl Biochem 4. Biotechnol. 2024

16. Madalyn Brown, Salahuddin Ahmed. Emerging role of proprotein convertase subtilisin/kexin type-9 (PCSK-9) in inflammation and diseases. Toxicol Appl Pharmacol. 2019; 370: 170-177.

17. Amritanshu S Pandey, Harpreet S Bajaj, Vinay Garg, Avinash Pandey, Subodh Verma. The emerging role of proprotein convertase subtilisin/kexin type-9 inhibition in secondary prevention: from clinical trials to real-world experience. Curr Opin Cardiol. 2017; 32: 633-641.

18. Vasilios Papademetriou, Konstantinos Stavropoulos, Christodoulos Papadopoulos, Konstantinos Koutsampasopoulos, Kiriakos Dimitriadis, Kostas Tsioufis. Role of PCSK9 Inhibitors in High Risk Patients with Dyslipidemia: Focus on Familial Hypercholesterolemia. Curr Pharm Des. 2018; 24: 3647-3653.

19. Brian Tomlinson, Nivritti Gajanan Patil, Manson Fok, Christopher Wai Kei Lam. Role of PCSK9 Inhibitors in Patients with Familial Hypercholesterolemia. Endocrinol Metab (Seoul). 2021; 36: 279-295.

20. Nicola Ferri, Alberto Corsini, Cesare R Sirtori, Massimiliano Ruscica. Bococizumab for the treatment of hypercholesterolaemia. Expert Opin Biol Ther. 2017; 17: 909-910.

21. Murielle M Véniant, Renee Komorowski, Ping Chen, Shanaka Stanislaus, Katherine Winters, Todd Hager ,et al. Long-acting FGF21 has enhanced efficacy in diet-induced obese mice and in obese rhesus monkeys. Endocrinology. 2012; 153: 4192-4203.

22. Menglong Xu, Gaoxin Lei, Manman Chen, Ke Wang, Wenxiu Lv, Panpan Zhang, et al. Development of a novel, fully human, anti-PCSK9 antibody with potent hypolipidemic activity by utilizing phage display-based strategy. EBioMedicine. 2021; 65: 103250.

23. Michael M Page, Gerald F Watts. Evolocumab in the treatment of dyslipidemia: pre-clinical and clinical pharmacology. Expert Opin Drug Metab Toxicol. 2015; 11: 1505-1515.

24. Jennifer G Robinson, Michel Farnier, Michel Krempf, Jean Bergeron, Gérald Luc, Maurizio Averna, et al. Efficacy and safety of alirocumab in reducing lipids and cardiovascular events. N Engl J Med. 2015; 372: 1489-1499.

25. Radmila Micanovic, David W Raches, James D Dunbar, David A Driver, Holly A Bina, Craig D Dickinson, et al. Different roles of N- and C-termini in the functional activity of FGF21. J Cell Physiol. 2009; 219: 227-234.

26. Jiayi Wei, Yueyang Sun, Heming Wang, Tong Zhu, Li Li, Ying Zhou, et al. Designer cellular spheroids with DNA origami for drug screening. Sci Adv. 2024; 10: eado9880.

27. Xinyang Li, Meiniang Wang, Xinhua Zhang, Chuxin Liu, Haitao Xiang, Mi Huang, et al. The novel llama-human chimeric antibody has potent effect in lowering LDL-c levels in hPCSK9 transgenic rats. Clin Transl Med. 2020; 9: 16.

28. Rachid Essalmani, Elodie Weider, Jadwiga Marcinkiewicz, Ann Chamberland, Delia Susan-Resiga, Anna Roubtsova., et al. A single domain antibody against the Cys- and His-rich domain of PCSK9 and evolocumab exhibit different inhibition mechanisms in humanized PCSK9 mice. Biol Chem. 2018; 399: 1363-1374.

29. LaDonna Clark. GLP-1 receptor agonists: A review of glycemic benefits and beyond. JAAPA. 2024; 37: 1-4.

30. Theingi M Thway, Jagadeesh Aluri, Bojan Lalovic, Chean E Ooi, Nicholas Sauter, Dongyuan Xing, et al. Effect of E7777 Immunogenicity on Pharmacokinetics, Efficacy, and Safety in Adult Patients With Relapsed or Refractory Cutaneous T-Cell Lymphoma. Clin Transl Sci. 2025; 18: e70166.

31. Xiaoying Sun, Ziyang Cui, Qingyun Wang, Liu Liu, Xiaojie Ding, Jiao Wang, et al. Formation and clinical effects of anti-drug antibodies against biologics in psoriasis treatment: An analysis of current evidence. Autoimmun Rev. 2024; 23: 103530.